Carbohydrate Polymers 92 (2013) 545–554

Contents lists available at SciVerse ScienceDirect

Carbohydrate Polymers

journal homepage: www.elsevier.com/locate/carbpol

# In vitro evaluation on novel modified chitosan for targeted antitumor drug delivery

Ding Qu, Haijiao Lin, Nan Zhang, Jingwei Xue, Can Zhang*

*Center of Drug Discovery, State Key Laboratory of Natural Medicines, China Pharmaceutical University, Nanjing 210009, PR China*

ARTICLE INFO

*Article history:*
Received 6 April 2012
Received in revised form 29 August 2012
Accepted 29 August 2012
Available online 6 September 2012

*Keywords:*
Chitosan
Paclitaxel
Micelles
Cellular uptake
Tumor targeting

ABSTRACT

In this study, a novel amphiphilic copolymer designed as *N*-octyl-*N*-phthalyl-3,6-*O*-(2-hydroxypropyl) chitosan (OPHPC) were synthesized and then conjugated with folic acid (FA-OPHPC) to produce a targeted drug carrier for tumor-specific drug delivery. OPHPC and FA-OPHPC were characterized by FT-IR, $^{1}$H NMR, $^{13}$C NMR and elemental analysis. Paclitaxel (PTX) loaded OPHPC micelles (PTX-OPHPC) with well-defined spherical shape and homogeneous distribution exhibited drug-loading rate ranging from 33.6% to 45.3% and entrapment efficiency from 50.5% to 82.8%. In the cellular uptake studies, PTX-OPHPC brought about a significantly higher amount of PTX accumulated in human breast adenocarcinoma cell line (MCF-7 cells) compared with Taxol®. Moreover, the cellular uptake of PTX in PTX loaded FA-OPHPC micelles (PTX-FA-OPHPC) was 3.2-fold improved in comparison with that of PTX-OPHPC. The results revealed that OPHPC micelle might be a promising drug carrier for promoting PTX cellular uptake and FA-OPHPC micelle could be used as a potential tumor-targeted drug vector.



## 1. Introduction

Nowadays polymeric micelles have received tremendous attention over the past decades due to the applications in drug delivery (Felt, Buri, & Gurny, 1998; Huo et al., 2012; Rekha & Sharma, 2009; Saboktakin & Tabatabaie, 2010), diagnostic imaging (Trubetskoy, 1999), photodynamic therapy (Nishiyama, Morimoto, Jang, & Kataoka, 2009), combination chemotherapy (Kano et al., 2007) and so on. As some studies point out, chitosan-based carriers have become one of the most promising drug vectors that have gained increasing interest as a safe delivery system for improving the solubility of water-insoluble drugs (Amidi & Hennink, 2010). In recent years, a great number of amphiphilic chitosan derivates have been developed as drug carriers with various functional groups, such as hydrophobic groups (stearic acid (Ye et al., 2008), linoleic acid (Tan & Liu, 2009), cholic acid (Ngawhirunpat et al., 2009) and deoxycholic acid (Lee, Kim, Kwon, & Jeong, 2000)) and hydrophilic units (glycol (Kim et al., 2008), poly(β-malic acid) (Zhao et al., 2009), carboxymethyl (Wang et al., 2008)).

An ideal drug delivery system based on modified chitosan with optimized design and compositions should ensure proper size (<200 nm in diameter) for enhanced permeability and retention (EPR) effect; low critical micelle concentration (CMC) for better stability; enhancement on the solubility of water-insoluble drugs in aqueous system; nontoxicity against normal cells; high cellular uptake by tumor specific targeting (Leong et al., 1998; Maruyama, 2002; Yoo, Doshi, & Mitragotri, 2011). In our previous studies, *N*-octyl-*O*-sulfate chitosan (NOSC) and its derivates have been developed as a series of promising drug delivery systems by physically entrapping various hydrophobic antitumor drugs. Paclitaxel (PTX) loaded NOSC micelles had the similar antitumor efficacy as Taxol® but with lower toxicity in intravenous injection and higher bioavailability in oral administration (Mo, Jin, et al., 2011; Mo, Xiao, Sun, Zhang, & Ping, 2011; Zhang et al., 2008). In addition, we also developed PEGylated NOSC, *N*-alkyl-*N*-trimethyl chitosan (Zhang, Ping, Zhang, & Shen, 2003), *N*,*O*-acyl-*N*-trimethyl chitosan chloride (Chen, Ding, Qu, & Zhang, 2008) and *N*-octyl-*N*-(2-carboxyl-cyclohexamethenyl) chitosan (Liu, Li, Jiang, Zhang, & Ping, 2010) for drug delivery over past years.

Use of polymeric carriers is also gaining momentum in drug delivery for active tumor targeting (Backer et al., 2005; Li et al., 2004; Nasongkla et al., 2004; Szebeni, Muggia, & Alving, 1998). To date, taking advantage of different expression levels of certain protein between normal and tumor cells, a diverse range of pilot molecules for cell-specific drug delivery have been available. For instance, polymeric micelles conjugated with folic acid (Moghimi, Hunter, & Murray, 2001; Wang et al., 2010), galactose (Liu, Yu, Chen, Zhang, & Zhang, 2011; Wu et al., 2009), anisamide (Nakagawa, Ming, Huang, & Juliano, 2010), cNGR (Son, Singha, & Kim, 2010) and monoclonal antibody (Torchilin, Lukyanov, Gao, & Papahadjopoulos-Sternberg, 2003; Yu et al., 2009) showed more accessibility to certain tumor cells than respective non-targeted

* Corresponding author. Tel.: +86 025 83271171; fax: +86 025 83271171.
*E-mail address:* zhangcan@cpu.edu.cn (C. Zhang).

0144-8617/$ – see front matter © 2012 Elsevier Ltd. All rights reserved.
http://dx.doi.org/10.1016/j.carbpol.2012.08.112

micelles. However, the water solubility of carrier might decrease after linking with a number of hydrophobic ligands, which presented adverse effects on drug delivery. Therefore, good solubility of carriers in both water and organic solvent was a positive factor which enabled us to select appropriate interactions in more alternative solvents and enhance the reaction activity of further modification. Despite considerable efforts to excellent water solubility in developing drug delivery, little chitosan derivates with good solubility in organic system was reported in drug delivery field.

Herein we report our present study on preparation, characterization and in vitro evaluation of *N*-octyl-*N*-phthalyl-3,6-*O*-(2-hydroxypropyl) chitosan (OPHPC) (OPHPC) and folate-modified OPHPC (FA-OPHPC). By introducing phthalyl units, OPHPC obtained good solubility in organic solvents, which could be linked with hydrophobic targeting ligands such as folic acid readily. PTX was selected as model drug because of its outstanding antineoplastic efficiency against various cancers (Carney, 1996; Rowinsky, Eisenhauer, Chaudhry, Arbuck, & Donehower, 1993; Tishler, Geard, Hall, & Schiff, 1992). In this paper, we investigated the improvement on solubility of PTX in aqueous medium using modified chitosan and evaluated the enhancement on cellular uptake of PTX by PTX loaded OPHPC micelles (PTX-OPHPC) and PTX loaded FA-OPHPC micelles (PTX-FA-OPHPC). Moreover, the internalization mechanism of PTX-FA-OPHPC and PTX-OPHPC were studied.

## 2. Experimental

### 2.1. Materials

Chitosan was purchased from Nantong Shuanglin Biochemical Co. Ltd. (China), with a deacetylation degree of 92% and viscosity average molecular weight of 70 kDa. Phthalic anhydride, propylene oxide and folic acid were offered by Sinopharma group Co. Ltd. (Shanghai, China). PTX was obtained from Yew Pharmaceutical Co. Ltd. (Jiangsu, China). NP-40 Cell lysis buffer and BCA protein assay kit were provided by Beyotime Institute of Biotechnology (Jiangsu, China). Dulbecco's modified Eagle medium (D-MEM, high glucose), fetal bovine serum (FBS), penicillin-streptomycin solution, phosphate buffered saline (PBS) were purchased from Thermo Fisher Scientific Inc (HyClone®, USA). All other chemicals and reagents were analytical grade.

### 2.2. Synthesis of amphipathic chitosan derivatives

*N*-octyl-*N*-phthalyl-3,6-*O*-(2-hydroxypropyl) chitosan (OPHPC) was prepared by introducing octyl and phthalyl groups to $NH_2$ on C2 and 2-hydroxypropyl groups to OH on C3 and C6 of the glucosamine units in chitosan, respectively.

#### 2.2.1. Preparation of N-octyl chitosan (OC)

The suspension of Chitosan (1.0 g, 6 mmol) in 30 mL of methanol was stirred vigorously at room temperature for 30 min, then octanal (6 mL, 37 mmol) was dropped into the suspension and the mixture was stirred at the same temperature for 12 h. At the end of this time, $NaBH_4$ (380 mg, 10 mmol) was slowly added to the resulting pale-yellow mixture in batches. After stirring for further 24 h, the suspension was filtrated and the residue was washed with water, water/methanol (1/1, v/v), methanol and diethyl ether successively. The product was dried at 60 °C under vacuum overnight to obtain 1.87 g crude product as a pale-yellow solid.

#### 2.2.2. Synthesis of N-octyl-N-phthalyl chitosan (OPC)

OC (805 mg, 3.27 mmol) was dissolved in 5 mL of DMF at room temperature followed by addition of phthalic anhydride (663 mg, 4.48 mmol) under nitrogen atmosphere. The mixture was stirred at 90 °C for 6 h, then cooled to room temperature and poured into 20 mL water with mechanical agitation. The resulting solid was filtered and washed with 80 mL water, and dried to give 1.6 g of OPC.

#### 2.2.3. Synthesis of N-octyl-N-phthalyl-3,6-O-(2-hydroxypropyl) chitosan (OPHPC)

OPC (0.5 g, 1.65 mmol) was suspended in 2.5 mL 50% (W/W) sodium hydroxide solution, then 5 mL of DMF was added dropwise and the mixture were stirred vigorously at 40 °C for 1 h. Propylene oxide (5 mL, 71.6 mmol) was dropped into suspension slowly and kept stirring for 10 h. Then the reaction mixture was poured in 80 mL ice water with mechanical agitation, and then neutralized to pH 7 with 10% hydrochloric acid solution. The filtrated solution was dialyzed against distilled water for 3 days using a dialysis bag (Lvniao Co. Ltd, molecular weight cut-off range (MWCO) of 10,000). 120 mg pale yellow powder was obtained after freeze drying finally.

#### 2.2.4. Preparation of folic acid (FA) modified OPHPC (FA-OPHPC)

*2.2.4.1. Activation of FA (FA-NHS).* The synthesis was performed by a modified procedure according to reported literature (York et al., 2009). Briefly, FA (0.5 g, 1.14 mmol) was dissolved in 10 mL of DMSO with stirring until complete dissolving, and then *N*,*N*-dicyclohexyl carbodie (DCC) (2.34 g, 11.4 mmol) and *N*-hydroxy succinimide (NHS) (0.7 g, 6.1 mmol) were added to the FA solution. The solution was allowed to stir at room temperature in the dark for 24 h, and then filtered, washed with cold ether. The product was dried under vacuum to yield yellow solid (0.68 g, 94%).

*2.2.4.2. Synthesis of FA-OPHPC.* OPHPC (65.1 mg) was dissolved in 6 mL of DMSO with stirring for 30 min, and then FA-NHS (651 mg, 1.14 mmol) was added to the OPHPC solution. After stirring at room temperature under nitrogen for 48 h, the solution was poured into 60 mL of water with vigorously stirring, and filtrated solution was dialyzed in distilled water for 3 days with dialysis bag (MWCO of 10,000). The dialyzed solution was freeze-dried to obtain 72.1 mg auratus powder.

#### 2.2.5. Synthesis of N-octyl-N,O-(2-hydroxypropyl) chitosan (OHPC)

OC (1.23 g, 5 mmol) was suspended in 5 mL 50% (W/W) sodium hydroxide solution, then 5 mL of DMF was added dropwise and the mixture were stirred vigorously at 40 °C for 1 h. Propylene oxide (8 mL, 114.5 mmol) was dropped into suspension slowly and kept stirring for 12 h. Then the reaction mixture was poured in 80 mL deionized water with mechanical agitation, and then neutralized to pH 7 with 10% hydrochloric acid solution. The filtrated solution was dialyzed against distilled water for 3 days using a dialysis bag (MWCO of 10,000). 56 mg pale yellow powder was obtained after freeze drying finally.

### 2.3. Characteristic of chitosan derivatives and assay of physicochemical properties

#### 2.3.1. Fourier transform infrared spectroscopy (FT-IR)

FT-IR spectra was recorded with KBr pellets on a Fourier transform infrared spectrometer (Nicolet 2000) at room temperature.

#### 2.3.2. Nuclear magnetic resonance spectroscopy (NMR)

NMR spectra was recorded on a Bruker AVANCE-300 spectrometer operating at 300 MHz at room temperature.

*2.3.3. Elemental analysis*

Elemental analysis was performed on a Vario EL III elemental analyzer. According to the data, the DS of octyl, phthalyl, and 2-hydroxypropyl group was calculated.

*2.3.4. WAXD assay*

WAXD spectra was obtained with XD-3A powder diffraction meter with Cu Kα radiation at a voltage of 40 kV and a current of 30 mA. The scanning rate was 5°/min and the scanning range of $2\theta$ was from 5° to 40° at room temperature.

*2.3.5. TG analysis (TGA)*

TGA was reported on chitosan and chitosan derivates using a Netzsch TG 209 F1 Libra® Thermal Analyzer. Experiments were performed with samples under a dynamic nitrogen atmosphere flowing at a rate of 50 mL/min and at a heating rate of 10 °C/min.

*2.3.6. Measurement of critical micelle concentration (CMC)*

The CMC values of OPHPC, FA-OPHPC and OHPC were measured by surface tension instrument (DCAT 21, Dataphysics, Germany). The surface tension values of OPHPC at various concentrations range from 0.25 to 158 μg/mL were measured at room temperature. Then, a curve based on log *C* and surface tension as abscissa and ordinate respectively was plotted.

*2.3.7. Gel permeation chromatography (GPC) analysis*

The MW distribution of OPHPC was determined by GPC (Shimadzu, Kyoto, Japan) equipped with a refractive index detector (RID-10A, Shimadzu, Kyoto, Japan) and columns (G4000PWxl, TSK-GEL, TOSOH, Japan). Deionized water was used as eluent at flow rate of 1 mL/min. The column temperature was maintained at 35 °C.

*2.3.8. Solubility analysis*

50 mg of OPHPC was dissolved in 2 mL of deionized water, DMF and DMSO at 25 ± 2 °C, respectively. Samples were shaked vigorously every 5 min, and then observed turbidity after 30 min. Test samples with clear solution and no visible particular matter were regarded as dissolve totally.

*2.4. Preparation and characterization of PTX-OPHPC*

*2.4.1. PTX detecting*

PTX concentrations were measured by HPLC (Shimadzu, LC-2010A HT, Japan). The mobile phase was a mixture of methanol and water (75/25, v/v). The column was Diamond C18 (4.6 mm × 250 mm) with 5 μm particles. The samples were delivered at a flow rate of 1.0 mL/min and detected at a wave length of 227 nm. The column temperature was maintained at 30 °C and injected volume of the sample was 20 μL.

*2.4.2. Preparation of PTX-OPHPC*

PTX-OPHPC were prepared using dialysis method. Briefly, 6 mg of PTX in 222 μL ethanol was dropped into the solution of 10 mg of OPHPC in 2.5 mL water with magnetic stirring vigorously at room temperature. After the addition, the mixture was dialyzed against distilled water for 4 h at room temperature using dialysis membrane (10,000 MW cutoff) and this dialysis procedure was repeated at least three times after replacing dialysis medium. The micellar solution was filtered with a 0.22 μm pore-sized microfiltration membrane, and then the PTX concentration of micelles was analyzed by HPLC and the resulting solution was finally freeze-dried.

The PTX-loading rate and entrapment efficiency in micelles were calculated by the following equations:

$$\text{drug-loading rate}\,(\%) = \frac{C_1 \times V_1}{W_{\text{freeze-dried micelle}}} \times 100 \quad \text{(A.1)}$$

$$\text{entrapment efficiency}\,(\%) = \frac{C_2 \times V_2}{W_{\text{PTX}}} \times 100 \quad \text{(A.2)}$$

where $C_1$, $C_2$, $V_1$, $V_2$, $W_{\text{freeze-dried micelle}}$ and $W_{\text{PTX}}$ represented the PTX concentration of freeze-dried micelles reconstituted in water, the PTX concentration of micellar solution, the volume of freeze-dried micelles reconstituted in water, the volume of micellar solution, the weight of freeze-dried micelles and the weight of PTX added, respectively.

*2.4.3. Characterization of PTX-OPHPC*

The size and zeta potential of PTX-OPHPC were measured by a Zeta potential analyzer (Zeta Plus, Brookhaven, USA). TEM analysis was obtained with JEM-200CX (JEOL Ltd., Japan) and AFM study was performed by VEECO Dimension 3100 Atomic Force Microscope.

*2.5. Cells culture*

MCF-7 cells (or L-O2 cells) were obtained from the cell bank of Chinese Academy of Sciences. The cells were cultured in D-MEM (or 1640) with 10% (v/v) FBS, 100 U/mL penicillin and 100 μg/mL streptomycin in an incubator at 37 °C under an atmosphere of 5% $CO_2$ and 90% relative humidity. The cells were subcultivated every 4–5 days (at 80% confluence) using trypsin at a split ratio of 1:6.

*2.6. Cytotoxicity studies*

The cells were seeded at a density of $1 \times 10^5$ cells per well in 96-well plates (Costar, USA). After 80% confluence, the culture medium was removed and 200 μL of the following test solutions (100 μL of FBS free culture medium with 100 μL of samples at various concentrations) and negative control (100 μL of FBS free culture medium with 100 μL of culture medium) were added into the wells. After further cells culture for 24 h, 20 μL of 5 mg/mL (3-(4,5-dimethylthiazol-2-yl)-2,5-iphenyltetrazolium bromide (MTT) PBS solution was added into each well, and then the cells were stained at 37 °C for 4 h. Thereafter, the medium was removed, and the cells were mixed with 150 μL of DMSO. The absorbance was measured at 570 nm by an ELISA (Thermo Scientific, USA). Relative cell viability (*R*%) was calculated as follows:

$$R\% = \frac{\text{absorbance}_{\text{test}}}{\text{absorbance}_{\text{control}}} \times 100\% \quad \text{(B.1)}$$

*2.7. Cellular uptake studies*

In order to evaluate the enhancement on cellular uptake of PTX by OPHPC micelles and the active targeting property of FA-OPHPC micelles on MCF-7 cells. The following works were performed.

*2.7.1. MCF-7 cells enhanced accumulation of PTX by PTX-loaded modified chitosan micelles (PTX-M)*

The cells were seeded into 24-well plates at a proper density. After 24 h of incubation (at 80% confluence), the medium was removed. The cells were treated with different concentrations of PTX in PTX-OPHPC and PTX-FA-OPHOC respectively. 400 μL of test solutions were added in the well, and then removed after culturing at 37 °C for 2 h. Subsequently, the cells were washed by 4 °C PBS thrice, and cultured with 160 μL of NP-40 cell lysis buffer for 15 min. The contents of PTX in MCF-7 cells were tested by HPLC and the cells protein was detected by BCA protein assay kit. Uptake ratio (*U*%) was calculated as the following equation.

$$U\% = \frac{Q_{\text{PTX in cells}}}{Q_{\text{cells protein}}} \times 100\% \quad \text{(C.1)}$$

where $Q_{\text{PTX in cells}}$ and $Q_{\text{cells protein}}$ represented the amounts of PTX in MCF-7 cells and cells protein, respectively.

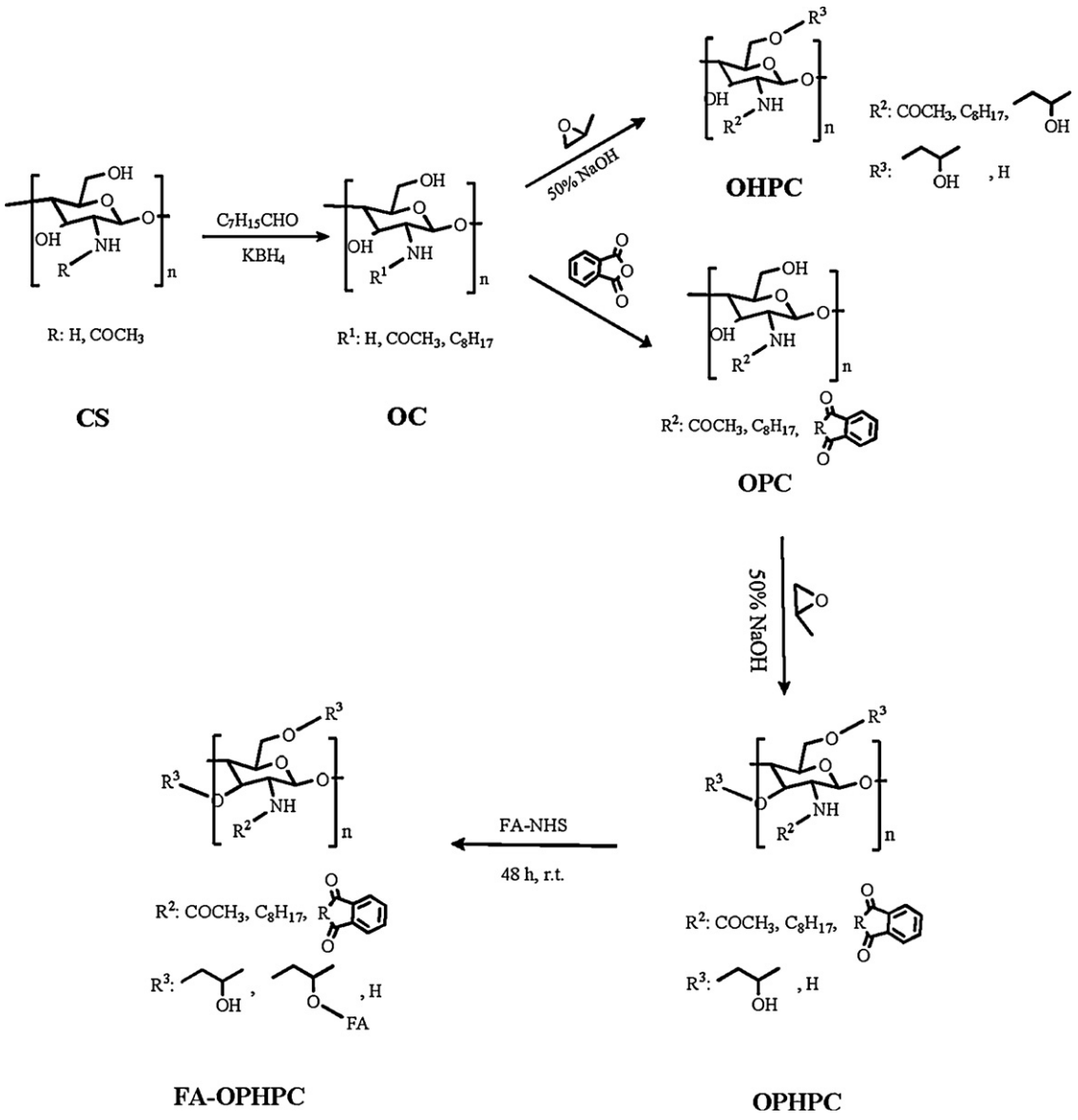


**Fig. 1.** Synthesis of OHPC, OPHPC and FA-OPHPC.

*2.7.2. Endocytosis pathways of PTX-M*

To investigate the endocytosis pathways of PTX-M, MCF-7 cells was pre-incubated with inhibitors of various endocytosis at safe concentrations for 30 min at 37 °C as follows: (1) inhibitor of folate receptor-mediated endocytosis: 441 μg/mL of folic acid, (2) inhibitor of clathrin-mediated endocytosis: 154 mg/mL of sucrose, (3) inhibitor of caveolae-mediated endocytosis: 54 μg/mL of genistein, (4) inhibitor of macropinocytosis: 133 μg/mL of amiloride. Following the pre-incubation, the cells were further treated with freshly prepared PTX-OPHPC and PTX-FA-OPHPC in the presence of the corresponding inhibitor for 2 h, respectively. Subsequently, the cells were washed with 4 °C PBS thrice, and the amounts of PTX in MCF-7 cells were assayed by HPLC and the cells protein were detected by BCA protein assay kit.

*2.8. Statistical analysis*

Data are given as mean ± S.D. Statistical significance was tested by two-tailed Student's *t*-test. Statistical significance was set at $^{*}P < 0.05$, and extremely significance was set at $^{**}P < 0.01$.

## 3. Results and discussion

*3.1. Synthesis and characterization of OPHPC and FA-OPHPC*

OPHPC was synthesized in a simple and controllable manner by covalently linking octyl, phthalyl and 2-hydroxypropyl groups with the backbone of chitosan; FA-OPHPC was prepared using a DCC/NHS conjugation method as presented in Fig. 1. The number-average molecular weight (Mn) of OPHPC was 330,000 measured utilizing GPC instrument. The solubilities of OPHPC in water, DMF and DMSO were more than 25 mg/mL.

The structures of chitosan derivatives were identified by FT-IR, $^{1}$H NMR and $^{13}$C NMR spectra.

Compared with chitosan (CS), as shown in Fig. 2(A), the characteristic peak (1594 $cm^{-1}$) representing amino groups deformation was weakened and the new peaks positioned at 2926, 2862 and 1385 $cm^{-1}$ were appeared, which suggested that octyl groups were introduced into amino groups of chitosan. The appearance of new intensive peaks at 1676 and 1620 $cm^{-1}$ could be attributed to the amide and benzene ring of phthalyl groups. The peak

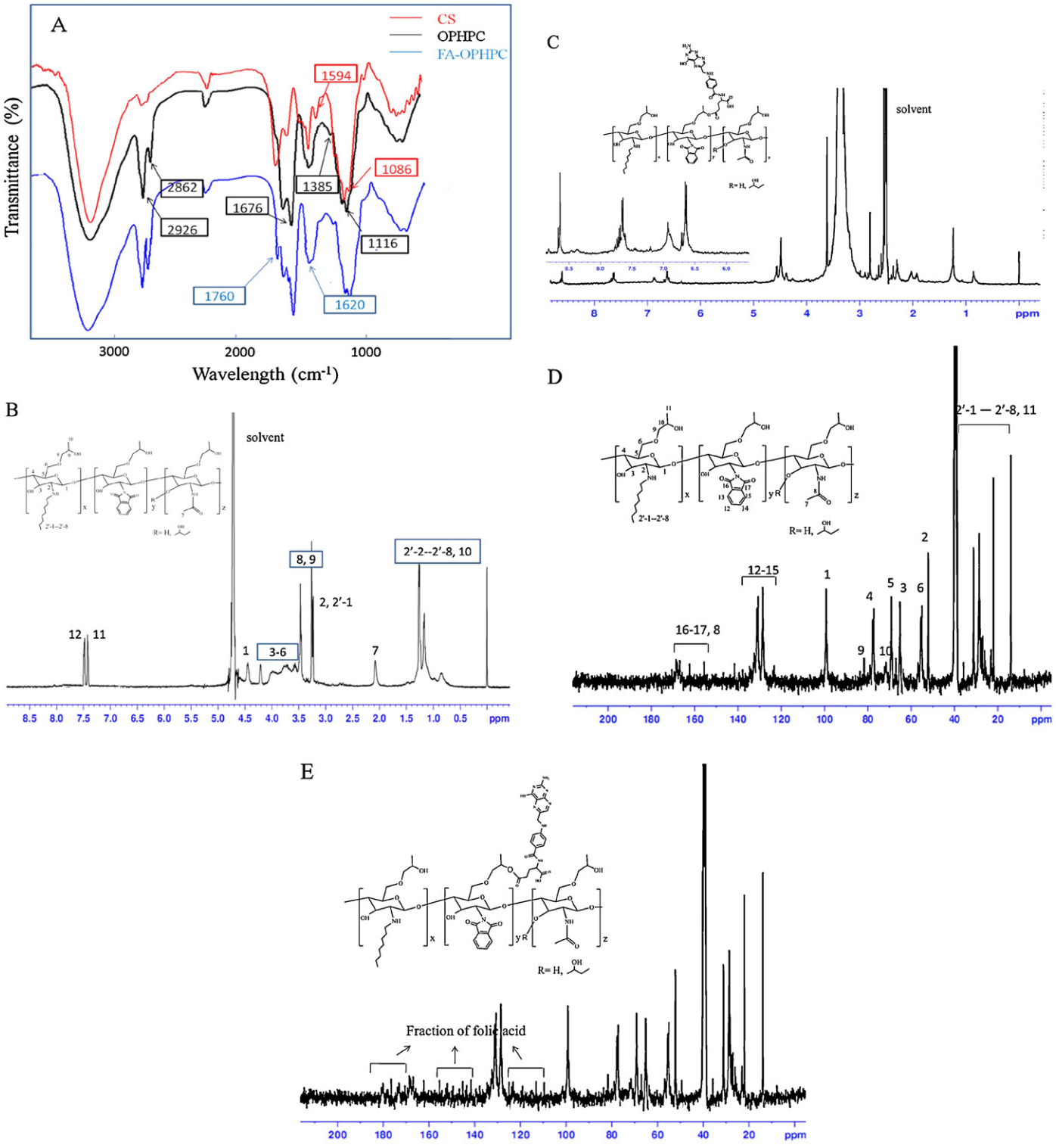


**Fig. 2.** Chemical structure characterization of OPHPC and FA-OPHPC. (A) FT-IR spectrum of chitosan and its derivatives, (B and C) $^{1}$H NMR spectrum of OPHPC and FA-OPHPC and (D and E) $^{13}$C NMR spectrum of OPHPC and FA-OPHPC.

at 1086 cm$^{-1}$ from 6-OH of chitosan was disappeared, and the new signal at 1116 cm$^{-1}$ was assigned to the 2-hydroxypropyl groups. It was indicated that 2-hydroxypropyl groups were mainly introduced into 6-OH groups of chitosan. All of these suggested that the OPHPC was synthesized successfully. Some new intensive peaks were observed in the FT-IR spectra of FA-OPHPC. The peak at about 1760 cm$^{-1}$ might represent the ester bond, and the signal at 1620 cm$^{-1}$ was attributed to the aromatic ring of the folate and phthalyl segments. These results confirmed that folate moieties were conjugated with OPHPC. The peaks of octyl and 2-hydroxypropyl groups were found in Fig. S1 (A), but no signal of phthalyl aromatic ring was detected. It suggested that the chemical structure of OHPC was in accordance with our design (see supplementary data, Fig. S1(A)).

Fig. 2(B and C) showed the $^1$H NMR spectra of OPHPC in $D_2O$ and FA-OPHPC in DMSO-d6. Fig. 2(B) depicted the $^1$H NMR spectrum of OPHPC, the signals at $\delta$ (ppm) 1.3–0.8 and 3.2 were assigned to the H of octyl segments. The peaks at $\delta$ (ppm) 7.5–7.4 were attributed to H11 and H12, which were identified that OPHPC contained phthalyl moieties. The signals at $\delta$ (ppm) 3.5–3.3 and 1.2 were attributed to H8, H9 and H10 of 2-hydroxypropyl groups. The peaks representing the backbone of chitosan were appeared at $\delta$ (ppm) 4.5–3.6 and 3.3, which were in accordance with the results from reported paper (Monier, Wei, Sarhan, & Ayad, 2010). The $^1$H NMR spectra of FA-OPHPC was shown in Fig. 2(C), chemical shifts from folate moieties were observed at $\delta$ (ppm) 8.6–6.6, which were assigned to the aromatic protons of folic acid, indicating the successful conjugation of FA moieties to chitosan. Moreover, the signal of phthalyl aromatic ring was not observed in Fig. S1 (B). It suggested that the OHPC was synthesized successfully (see supplementary data, Fig. S1 (B)).

Fig. 2(D and E) showed the $^{13}$C NMR spectra of OPHPC and FA-OPHPC. In Fig. 2(D), the signals at $\delta$ (ppm) 55.7, 58.1, 69.1, 71.1, 78.2 and 99.8 were detected, which were assigned to the C2, C6, C3, C5, C4 and C1 of chitosan, respectively. The peaks at $\delta$ (ppm) 40.5–14.8 might belong to the octyl groups, and the signals at $\delta$ (ppm) 131.5–128.1 were attributed to the phthalyl aromatic ring. The most specific carbon signals of amide were found at $\delta$ (ppm) 168–152. The peaks of 2-hydroxypropyl groups were detected at $\delta$ (ppm) 80.7, 67.7 and 26.4. In Fig. 2(E), the signals of aromatic ring from FA moieties were appeared at $\delta$ (ppm) 181.7–171.2, 153.7–142.5 and 126.3–110.2. All of these results indicated that the chemical structures of OPHPC and FA-OPHPC were certified.

The DS of various groups were calculated by comparing the C and N molar ratio obtained by elemental analysis for each chitosan derivative. The increase in the molar ratio suggested the increasing carbon in monosaccharide of chitosan chain, since each constitutional repeating unit included only one nitrogen (Miwa et al., 1998). In our previous researches, DS of octyl groups at 60% exhibited the best drug loading capacity (Yao, Zhang, Ping, & Yu, 2007). To investigate the influence of physicochemical properties on OPHPC with various DS of phthalyl and 2-hydroxypropyl groups, we controlled different DS of phthalyl and 2-hydroxypropyl groups by varying reaction time. In addition, the DS of each substituent group examined as the following equations:

$$\text{DS of octyl groups} = \text{C/N (mol)}_{\text{OC}} - \text{C/N(mol)}_{\text{chitosan}} \quad \text{(D.1)}$$

$$\text{DS of phthalyl groups} = \text{C/N (mol)}_{\text{OPC}} - \text{C/N(mol)}_{\text{OC}} \quad \text{(D.2)}$$

$$\text{DS of 2-hydroxypropyl groups} = \text{C/N(mol)}_{\text{OPHPC}} - \text{C/N(mol)}_{\text{OPC}} \quad \text{(D.3)}$$

The final DS of octyl, phthalyl, 2-hydroxypropyl and FA groups at 0.6, 0.29, 1.06 and 0.05 were used in the cellular studies, respectively.

The crystallization of chitosan, OPHPC and FA-OPHPC were assayed by WAXD pattern as presented in Fig. 3(A). Chitosan had two reflections appearing at $2\theta = 5^\circ$ and $20^\circ$. It is clear that peaks of OPHPC and FA-OPHPC decrease at $2\theta = 5^\circ$ and $20^\circ$ followed by incorporation of substituent groups into the amino and hydroxyl of chitosan. It indicated that chitosan might decrease the ability of forming intermolecular hydrogen bonds and then result in being amorphous after introduction of various groups, which corresponded to the results reported by previous study (Li et al., 2009).

The TGA spectra of chitosan, OPHPC and FA-OPHPC were shown in Fig. 3(B). Chitosan showed slow weight loss starting from 60 to 250 °C due to the decomposition of polymer with low molecular weight. Because most of the polymers with low molecular weight were removed by dialysis, OPHPC and FA-OPHPC exhibited a slow weight loss up to about 100 °C which might result from the presence of moisture, but no weight loss occurred at the later stage. However, a rapid weight loss was observed between 250 and 300 °C, which was attributed to the abolition of octyl, phthalyl and 2-hydroxypropyl segments. The following weight loss after 300 °C was assigned to the decomposing of chitosan backbone (Yao et al., 2007).

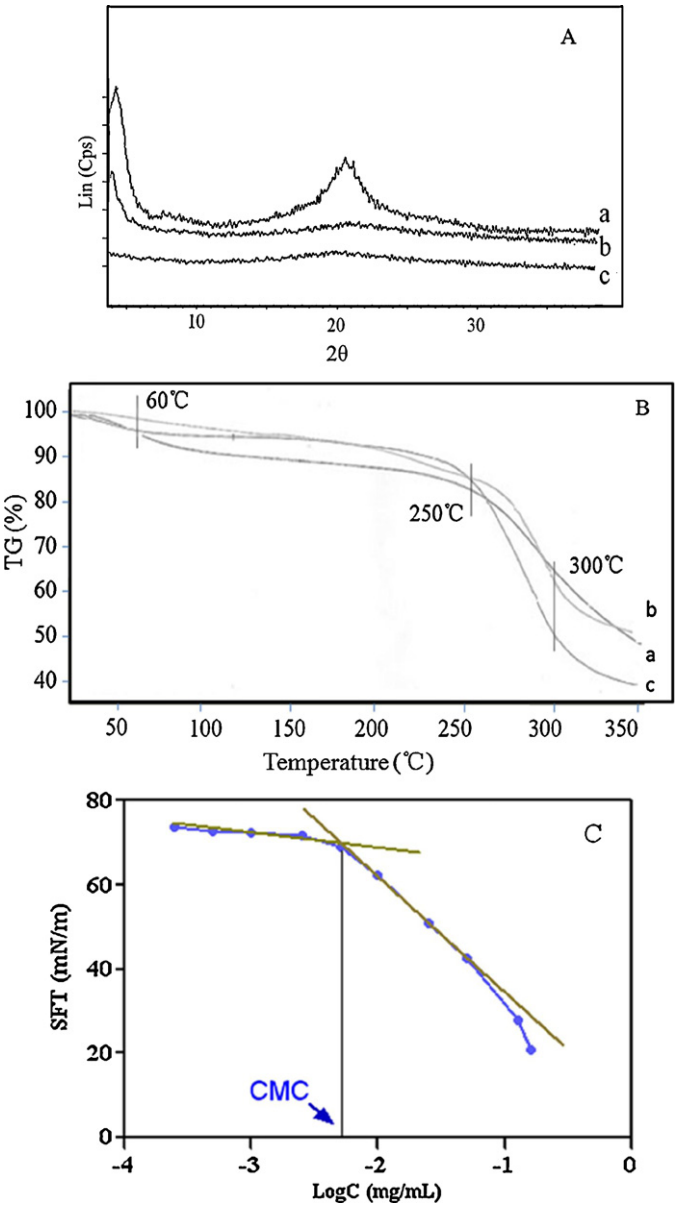


**Fig. 3.** Physiochemical properties of chitosan derivatives. (A) Patterns of WAXD patterns of (a) chitosan, (b) OPHPC and (c) FA-OPHPC, (B) TGA images of (a) chitosan, (b) OPHPC and (c) FA-OPHPC, (C) the plot of surface tension vs log *C* for OPHPC in water at 25 °C (DS of octyl, phthalyl and 2-hydroxypropyl groups are 0.60, 0.29 and 1.06, respectively).

### 3.2. CMC characteristics

In our previous study, phthalated chitosan presented a perfect solubility in organic solvents. We inferred from such phenomena that water-soluble chitosan derivates might also obtain excellent solubility in organic solvents after incorporation of phthalyl groups. Therefore, phthalyl groups were linked with $NH_2$ of chitosan and

**Table 1**
Formulation characterizations of PTX-OPHPC with different ratios of PTX and OPHPC (W/W).

| PTX/OPHPC (W/W) | Size (nm) | PI | Zeta (mV) | DEE (%) | DLE (%) |
|---|---|---|---|---|---|
| 2/10 | 106.2 ± 0.8 | 0.134 ± 0.015 | −24.83 ± 1.04 | 51.8 ± 0.9 | 34.1 ± 0.7 |
| 4/10 | 103.6 ± 0.4 | 0.107 ± 0.01 | −26.43 ± 1.59 | 50.5 ± 1.7 | 33.6 ± 1.3 |
| 6/10 | 104.2 ± 0.7 | 0.133 ± 0.017 | −25.78 ± 2.48 | 77.3 ± 1.1 | 43.6 ± 0.8 |
| 8/10 | 133.2 ± 1.2 | 0.171 ± 0.004 | −29.69 ± 1.22 | 74.7 ± 0.9 | 42.8 ± 0.5 |
| 10/10 | 153.1 ± 0.9 | 0.175 ± 0.023 | −29.57 ± 1.23 | 82.8 ± 1.4 | 45.3 ± 1.2 |

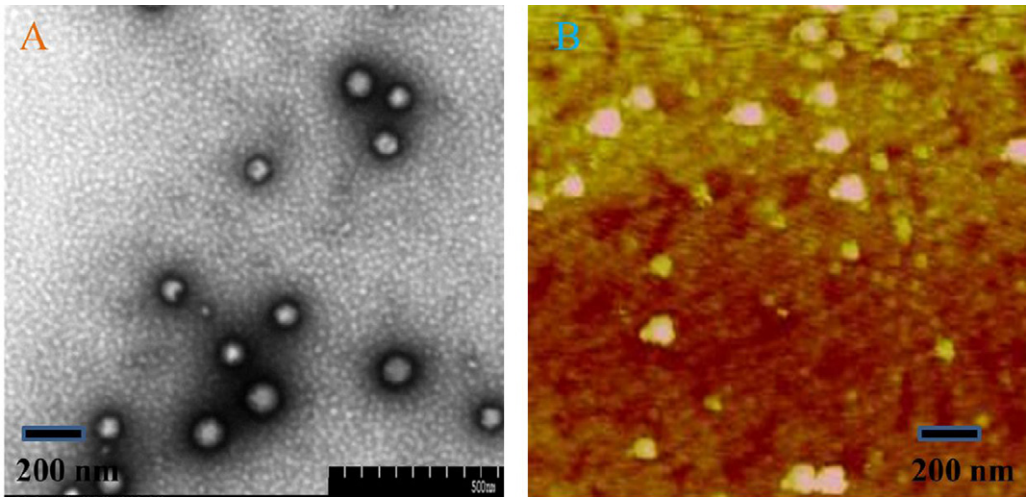


**Fig. 4.** Morphologic patterns: (A) TEM and (B) AFM images of PTX-OPHPC.

controlled at DS of 29%. The CMC values of OPHPC and OHPC were analyzed by surface tension method to evaluate the aggregation behavior of OPHPC in deionized water and identify the contribution of phthalyl groups in CMC performance. The plot of surface tension against log *C* for OPHPC in water at 25 °C was shown in Fig. 3(C). The concentration corresponding to the point of intersection on the curve represented CMC value of OPHPC, which was calculated to be 7.7 μg/mL. However, OHPC might not form micelles because the surface tension of OHPC had no significant change at test concentration range from 6.4 to 400 μg/mL, which indicated that 29% of phthalyl was necessary to obtain a low CMC for OPHPC (see supplementary data, Fig. S2 (A)). In this study, OPHPC can self-assemble micelles easily in aqueous solution at relatively low concentration, which suggested that our materials might endure the dilution in vivo potentially. The CMC of FA-OPHPC was also detected to be about 8 μg/mL by the same method, showing a similar result to that of OPHPC (see supplementary data, Fig. S2 (B)).

### 3.3. Preparation and characterization of PTX-OPHPC and PTX-FA-OPHPC

PTX-OPHPC and PTX-FA-OPHPC were prepared by general dialysis method at room temperature. The size and zeta potential of PTX-OPHPC and PTX-FA-OPHPC were analyzed with dynamic light scattering (DLS) at room temperature. As shown in Table 1, various feeding ratios of the drug to carrier (W/W) showed different performances in size, zeta potential, drug-loading efficiency (DLE) and drug-encapsulating efficiency (DEE). Finally, the PTX-OPHPC formula with feeding ratio of PTX to OPHPC, which exhibited a small particle size, relative high DLE and DEE, was decided to be 6/10 in following studies. Furthermore, TEM and AFM images in Fig. 4 showed that PTX-OPHPC were nearly spherical with average size as well as narrow distribution and dispersed homogeneously in aqueous medium, which accorded with the results from DLS. PTX-FA-OPHPC showed similar behavior to PTX-OPHPC in the morphological studies (see supplementary data, Fig. S3).

When the degrees of crystallization of polymer increased, conformations were more stable (Yao et al., 2007). It suggested that the drug-loaded capability of OPHPC were highly relative to crystallization of carrier. The evidence could be observed in Fig. 3(A), OPHPC and FA-OPHPC displayed good solubilization of PTX because chitosan modifications could rotate their backbones more easily than chitosan. In addition, lower crystallization might promote the affinity between the inner part of micelles and hydrophobic drugs.

### 3.4. Cytotoxicity studies

To investigate the potential cytotoxicity against the normal cell lines and the influence of phthalyl groups in cytotoxicity, the antiproliferation of OHPC, OPHPC and FA-OPHPC were gauged using MTT assay. As shown in Fig. 5, OPHPC and FA-OPHPC displayed little cytotoxicity against L-O2 cells with the concentration from 31.25 to 500 μg/mL. Furthermore, no remarkable difference in the

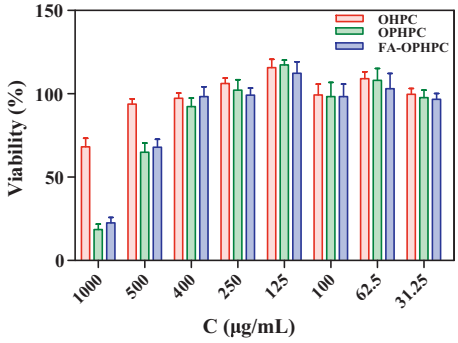


**Fig. 5.** Cytotoxicity of OHPC (DS of octyl and 2-hydroxypropyl groups are 60% and 106%, respectively), OPHPC (DS of octyl, phthalyl and 2-hydroxypropyl groups are 60%, 29% and 106%, respectively) and FA-OPHPC (DS of octyl, phthalyl, 2-hydroxypropyl and FA groups are 60%, 29%, 106% and 5%, respectively) against L-O2 cell line at various concentrations ($n = 6$).

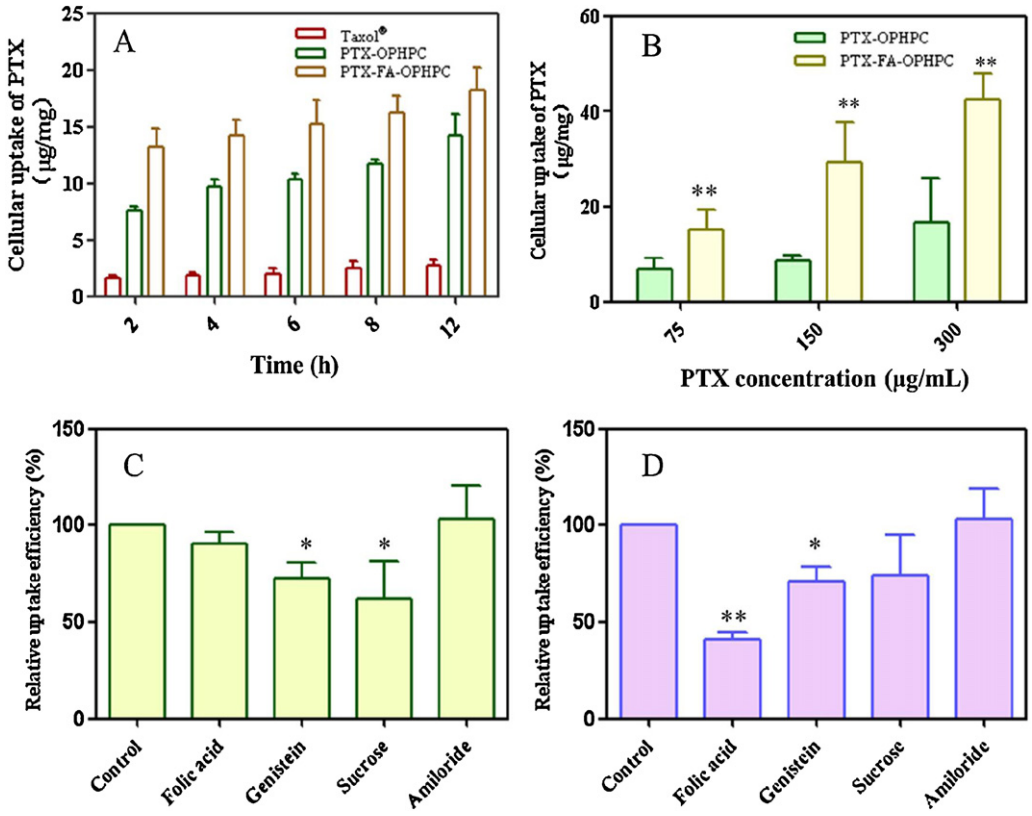


**Fig. 6.** MCF-7 cellular uptake studies. MCF-7 cellular uptake of PTX: (A) at different time with 50 μg/mL PTX ($n = 3$), (B) with 75, 150 and 300 μg/mL PTX for 2 h ($n = 6$, $^{**}P < 0.01$ vs PTX-OPHPC at the same time). Relative uptake efficiency of PTX-M: (C) PTX-OPHPC and (D) PTX-FA-OPHPC with 50 μg/mL PTX in the absence or presence of various endocytosis inhibitors ($n = 3$; $^{*}P < 0.05$, $^{**}P < 0.01$ vs control).

cytotoxicity of OPHPC and FA-OPHPC at the same concentration was observed, suggesting that FA moieties did not influence the cytotoxicity. Although incorporation of phthalyl groups was critical to improve the solubility of chitosan modifications and kept an excellent drug-loaded capability, OHPC displayed a lower cytotoxicity against L-O2 cells in comparison with OPHPC, indicating the increase of cytotoxicity after introduction of phthalyl groups. These results demonstrated that OPHPC and FA-OPHPC were persuasive for the potential application as safe drug vehicles.

### 3.5. Cellular uptake studies

#### 3.5.1. MCF-7 cells accumulation of PTX

Based on the natural high affinity of folate receptor protein (FR), which is commonly over-expressed on the surface of many human tumor cells such as brain, kidney, lung, and breast tumor cells, folate-modified carrier would bind tightly to the FR and trigger cellular uptake via receptor-mediated endocytosis (Goldstein, Anderson, & Brown, 1979), MCF-7 cell line was chosen as the over-expressed FR cell models for the following studies.

In the cellular uptake studies, the uptake of PTX in Taxol®, PTX-OPHPC and PTX-FA-OPHPC by MCF-7 cells were assayed to evaluate the uptake enhancement and potential ability of active targeting to tumor cells. The cellular uptake kinetics were studied and results were displayed in Fig. 6(A), PTX-OPHPC, PTX-FA-OPHPC and Taxol® represented time-dependent pathway in cellular uptake and indicated that PTX-M had a strong effect on promoting the MCF-7 cellular uptake of PTX. In Fig. 6(B), MCF-7 cellular uptake of PTX with 300, 150 and 75 μg/mL concentration of PTX-FA-OPHPC were $42.64 \pm 5.35$, $29.38 \pm 8.32$ and $15.23 \pm 4.23$ μg/mg, which were 2.55-fold, 3.4-fold, and 2.22-fold higher than that of PTX-OPHPC at the same concentration of PTX, respectively ($^{**}P < 0.01$), suggesting that PTX-FA-OPHPC could act as an efficiently active targeted drug delivery system in comparison with PTX-OPHPC.

#### 3.5.2. Endocytosis pathways of PTX-M

Surface chemistry of micelles greatly impacts on endocytosis pathway. Modulating the potential, shape, size and surface modification of the particles could realize a specific internalization pathway, such as the clathrin-mediated, caveolae-mediated or receptor-mediated endocytosis (Lee et al., 2000; Maruyama, 2002). In an effort to elucidate the potential uptake mechanisms involved in the cellular uptake of the test micelles, the sucrose, genistein, folic acid and amiloride were acted as the specific agents for clathrin-mediated, caveolae-mediated, folate receptor-mediated endocytosis and macropinocytosis respectively to investigate each type of cellular uptake mechanism. As shown in Fig. 6(C and D), in comparison with MCF-7 cellular uptake of PTX-M with 50 mg/mL PTX without any endocytosis inhibitors as control, it demonstrated that different endocytosis inhibitors presented different effects on internalization of micelles into MCF-7 cells. Incubation of MCF-7 cells with PTX-OPHPC in the presence of sucrose or genistein resulted in the significant ($^{*}P < 0.05$) decrease of cellular uptake of PTX, indicating that clathrin and caveolin were involved in the internalization of PTX-OPHPC. However, after culture of PTX-FA-OPHPC and folic acid with MCF-7 cells for 1 h, the cellular uptake of PTX was extremely significant ($^{**}P < 0.01$) inhibited, suggesting that PTX-FA-OPHPC could entry cells through folate receptor-mediated pathway. Meanwhile, the cellular uptake of PTX was decreased about 22% after treating with genistein, suggesting that the endocytosis mechanism of folate conjugated micelles as a tumor targeting drug delivery system also carried drugs into tumor cells via the caveolae-mediated pathway, and such results were in accordance

with the previous papers (Wang, Tiruppathi, Cho, Minshall, & Malik, 2011).

## 4. Conclusions

In this paper, OPHPC and FA-OPHPC were designed and synthesized. The chemical structures and some physical properties were characterized by $^{1}$H NMR, $^{13}$C NMR, FT-IR, elemental analysis, WAXD, GPC and TGA. The CMC and solubility of OPHPC in water and organic solvents were improved by introducing phthalyl groups. PTX-OPHPC with small particle size and narrow distribution were prepared, which showed that the apparent solubility of PTX was increased by 4000-fold in comparison with that of free PTX in aqueous medium. OPHPC and FA-OPHPC showed nearly noncytotoxicity against L-O2 cells. In the cellular studies, PTX-FA-OPHPC significantly improved the uptake of PTX compared with PTX-OPHPC and Taxol®. Furthermore, we also illustrated that folate moieties exhibited a direct impact on the internalization mechanism. PTX-FA-OPHPC entered MCF-7 cells via folate receptor-mediated and caveolae-mediated pathways, while the internalization of PTX-OPHPC via clathrin-mediated and caveolae-mediated pathways were observed. In conclusion, it suggested that PTX-OPHPC exhibited significant enhancement on cellular uptake and PTX-FA-OPHPC displayed a good active targeting ability to MCF-7 cells.

## Acknowledgements

This study is financially supported by Ph.D. Programs Foundation of Ministry of Education of China, 20090096110005 and 111 Project from the Ministry of Education of China the State Administration of Foreign Expert Affairs of China (No. 111-2-07).

## Appendix A. Supplementary data

Supplementary data associated with this article can be found, in the online version, at http://dx.doi.org/10.1016/j.carbpol.2012.08.112.

## References

Amidi, M., & Hennink, W. E. (2010). Chitosan-based formulations of drugs, imaging agents and biotherapeutics. *Advanced Drug Delivery Reviews*, *62*, 1–2.

Backer, M. V., Gaynutdinov, T. I., Patel, V., Bandyopadhyaya, A. K., Thirumamagal, B. T., Tjarks, W., et al. (2005). Vascular endothelial growth factor selectively targets boronated dendrimers to tumor vasculature. *Molecular Cancer Therapeutics*, *4*, 1423–1429.

Carney, D. N. (1996). Chemotherapy in the management of patients with inoperable non-small cell lung cancer. *Seminars in Oncology*, *23*, 71–75.

Chen, X. L., Ding, S., Qu, G. W., & Zhang, C. (2008). Synthesis of novel chitosan derivatives for micellar solubilization of Cyclosporine A. *Journal of Bioactive and Compatible Polymers*, *23*, 563–578.

Felt, O., Buri, P., & Gurny, R. (1998). Chitosan: A unique polysaccharide for drug delivery. *Drug Development and Industrial Pharmacy*, *24*, 979–993.

Goldstein, J. L., Anderson, R. G., & Brown, M. S. (1979). Coated pits, coated vesicles and receptor-mediated endocytosis. *Nature*, *279*, 679–685.

Huo, M., Zou, A., Yao, C., Zhang, Y., Zhou, J., Wang, J., et al. (2012). Somatostatin receptor-mediated tumor-targeting drug delivery using octreotide-PEG-deoxycholic acid conjugate-modified N-deoxycholic acid-O. *N-hydroxyethylation chitosan micelles. Biomaterials*, *33*(27), 6393–6407.

Kano, M. R., Bae, Y., Iwata, C., Morishita, Y., Yashiro, M., Oka, M., et al. (2007). Improvement of cancer-targeting therapy, using nanocarriers for intractable solid tumors by inhibition of TGF-beta signaling. *Proceedings of the National Academy of Sciences of the United States of America*, *104*, 3460–3465.

Kim, J. H., Kim, Y. S., Park, K., Lee, S., Nam, H. Y., Min, K. H., et al. (2008). Antitumor efficacy of cisplatin-loaded glycol chitosan nanoparticles in tumor-bearing mice. *Journal of Controlled Release*, *127*, 41–49.

Lee, K. Y., Kim, J. H., Kwon, I. C., & Jeong, S. Y. (2000). Self-aggregates of deoxycholic acid-modified chitosan as a novel carrier of adriamycin. *Colloid and Polymer Science*, *278*, 1216–1219.

Leong, K. W., Mao, H. Q., Truong-Le, V. L., Roy, K., Walsh, S. M., & August, J. T. (1998). DNA-polycation nanospheres as non-viral gene delivery vehicles. *Journal of Controlled Release*, *53*, 183–193.

Li, L., Wartchow, C. A., Danthi, S. N., Shen, Z., Dechene, N., Pease, J., et al. (2004). A novel antiangiogenesis therapy using an integrin antagonist or anti-FLK-1 antibody coated 90 Y-labeled nanoparticles. *International Journal of Radiation Oncology Biology and Physics*, *58*, 1215–1227.

Li, Q., Yang, D., Ma, G., Xu, Q., Chen, X., Lu, F., et al. (2009). Synthesis and characterization of chitosan-based hydrogels. *International Journal of Biological Macromolecules*, *44*, 121–127.

Liu, J., Li, H., Jiang, X., Zhang, C., & Ping, Q. (2010). Novel pH-sensitive chitosan-derived micelles loaded with paclitaxel. *Carbohydrate Polymers*, *82*, 432–439.

Liu, C., Yu, W., Chen, Z., Zhang, J., & Zhang, N. (2011). Enhanced gene transfection efficiency in CD13-positive vascular endothelial cells with targeted poly(lactic acid)–poly(ethylene glycol) nanoparticles through caveolae-mediated endocytosis. *Journal of Controlled Release*, *151*, 162–175.

Maruyama, K. (2002). PEG-immunoliposome. *Bioscience Reports*, *22*(2), 251–266.

Miwa, A., Ishibe, A., Nakano, M., Yamahira, T., Itai, S., Jinno, S., et al. (1998). Development of novel chitosan derivatives as micellar carriers of taxol. *Pharmaceutical Research*, *15*, 1844–1850.

Mo, R., Jin, X., Li, N., Ju, C., Sun, M., Zhang, C., et al. (2011). The mechanism of enhancement on oral absorption of paclitaxel by *N*-octyl-*O*-sulfate chitosan micelles. *Biomaterials*, *32*, 4609–4620.

Mo, R., Xiao, Y., Sun, M., Zhang, C., & Ping, Q. (2011). Enhancing effect of *N*-octyl-*O*-sulfate chitosan on etoposide absorption. *International Journal of Pharmaceutics*, *409*, 38–45.

Moghimi, S. M., Hunter, A. C., & Murray, J. C. (2001). Long-circulating and target-specific nanoparticles: Theory to practice. *Pharmacological Reviews*, *53*, 283–318.

Monier, M., Wei, Y., Sarhan, A. A., & Ayad, D. M. (2010). Synthesis and characterization of photo-crosslinkable hydrogel membranes based on modified chitosan. *Polymer*, *51*, 1002–1009.

Nakagawa, O., Ming, X., Huang, L., & Juliano, R. L. (2010). Targeted intracellular delivery of antisense oligonucleotides via conjugation with small-molecule ligands. *Journal of the American Chemical Society*, *132*, 8848–8849.

Nasongkla, N., Shuai, X., Ai, H., Weinberg, B., Pink, J., Boothman, D. A., et al. (2004). cRGD-functionalized polymer micelles for targeted doxorubicin delivery. *Angewandte Chemie International Edition*, *43*, 6323–6327.

Ngawhirunpat, T., Wonglertnirant, N., Opanasopit, P., Ruktanonchai, U., Yoksan, R., Wasanasuk, K., et al. (2009). Incorporation methods for cholic acid chitosan-g-mPEG self-assembly micellar system containing camptothecin. *Colloids Surfaces B: Biointerfaces*, *74*, 253–259.

Nishiyama, N., Morimoto, Y., Jang, W. D., & Kataoka, K. (2009). Design and development of dendrimer photosensitizer-incorporated polymeric micelles for enhanced photodynamic therapy. *Advanced Drug Delivery Reviews*, *61*, 327–338.

Rekha, M. R., & Sharma, C. P. (2009). Synthesis and evaluation of lauryl succinyl chitosan particles towards oral insulin delivery and absorption. *Journal of Controlled Release*, *135*(2), 144–151.

Rowinsky, E. K., Eisenhauer, E. A., Chaudhry, V., Arbuck, S. G., & Donehower, R. C. (1993). Clinical toxicities encountered with Paclitaxel (Taxol). *Seminar in Oncology*, *20*, 1–15.

Saboktakin, M. R., & Tabatabaie, R. (2010). Synthesis and characterization of superparamagnetic chitosan-dextran sulfate hydrogels as nano carriers for colon-specific drug delivery. *Carbohydrate Polymers*, *81*, 372–376.

Son, S., Singha, K., & Kim, W. J. (2010). Bioreducible BPEI-SS-PEG-cNGR polymer as a tumor targeted nonviral gene carrier. *Biomaterials*, *31*, 6344–6354.

Szebeni, J., Muggia, F. M., & Alving, C. R. (1998). Complement activation by cremophor EL as a possible contributor to hypersensitivity to paclitaxel: An in vitro study. *Journal of the National Cancer Institute*, *90*, 300–306.

Tan, Y. L., & Liu, C. G. (2009). Self-aggregated nanoparticles from linoleic acid modified carboxymethyl chitosan: Synthesis, characterization and application in vitro. *Colloids Surfaces B: Biointerfaces*, *69*, 178–182.

Tishler, R. B., Geard, C. R., Hall, E. J., & Schiff, P. B. (1992). Taxol sensitizes human astrocytoma cells to radiation. *Cancer Research*, *52*, 3495–3497.

Torchilin, V. P., Lukyanov, A. N., Gao, Z., & Papahadjopoulos-Sternberg, B. (2003). Immunomicelles: Targeted pharmaceutical carriers for poorly soluble drugs. *Proceedings of the National Academy of Sciences of the United States of America*, *100*, 6039–6044.

Trubetskoy, V. S. (1999). Polymeric micelles as carriers of diagnostic agents. *Advanced Drug Delivery Reviews*, *37*, 81–88.

Wang, Y. S., Jiang, Q., Li, R. S., Liu, L. L., Zhang, Q. Q., Wang, Y. M., et al. (2008). Self-assembled nanoparticles of cholesterol-modified *O*-carboxymethyl chitosan as a novel carrier for paclitaxel. *Nanotechnology*, *19*, 145101.

Wang, H., Zhao, P., Liang, X., Gong, X., Song, T., Niu, R., et al. (2010). Folate-PEG coated cationic modified chitosan—Cholesterol liposomes for tumor-targeted drug delivery. *Biomaterials*, *31*, 4129–4138.

Wang, Z., Tiruppathi, C., Cho, J., Minshall, R. D., & Malik, A. B. (2011). Delivery of nanoparticle-complexed drugs across the vascular endothelial barrier via caveolae. *IUBMB Life*, *63*(8), 659–667.

Wu, D. Q., Lu, B., Chang, C., Chen, C. S., Wang, T., & Zhang, Y. Y. (2009). Galactosylated fluorescent labeled micelles as a liver targeting drug carrier. *Biomaterials*, *30*, 1363–1371.

Yao, Z., Zhang, C., Ping, Q., & Yu, L. (2007). A series of novel chitosan derivatives: Synthesis, characterization and micellar solubilization of paclitaxel. *Carbohydrate Polymers*, *68*, 781–792.

Ye, Y. Q., Yang, F. L., Hu, F. Q., Du, Y. Z., Yuan, H., & Yu, H. Y. (2008). Core-modified chitosan-based polymeric micelles for controlled release of doxorubicin. *International Journal of Pharmaceutics*, *352*, 294–301.

Yoo, J. W., Doshi, N., & Mitragotri, S. (2011). Adaptive micro and nanoparticles: Temporal control over carrier properties to facilitate drug delivery. *Advanced Drug Delivery Reviews*, *63*, 1247–1256.

York, A. W., Zhang, Y., Holley, A. C., Guo, Y., Huang, F., & McCormick, C. L. (2009). Facile synthesis of multivalent folate-block copolymer conjugates via aqueous RAFT polymerization: Targeted delivery of siRNA and subsequent gene suppression. *Biomacromolecules*, *10*, 936–943.

Yu, W., Liu, C., Ye, J., Zou, W., Zhang, N., & Xu, W. (2009). Novel cationic SLN containing a synthesized single-tailed lipid as a modifier for gene delivery. *Nanotechnology*, *20*, 215102.

Zhang, C., Ping, Q., Zhang, H., & Shen, J. (2003). Preparation of *N*-alkyl-*O*-sulfate chitosan derivatives and micellar solubilization of taxol. *Carbohydrate Polymers*, *54*, 137–141.

Zhang, C., Qu, G., Sun, Y., Wu, X., Yao, Z., Guo, Q., et al. (2008). Pharmacokinetics, biodistribution, efficacy and safety of *N*-octyl-*O*-sulfate chitosan micelles loaded with paclitaxel. *Biomaterials*, *29*, 1233–1241.

Zhao, Z., He, M., Yin, L., Bao, J., Shi, L., Wang, B., et al. (2009). Biodegradable nanoparticles based on linoleic acid and poly(β-malic acid) double grafted chitosan derivatives as carriers of anticancer drugs. *Biomacromolecules*, *10*, 565–572.